Progress towards quantum-enhanced interferometry with harmonically trapped quantum matter-wave bright solitons

Bettina Gertjerenken[*]
Department of Mathematics and Statistics, University of Massachusetts Amherst, Amherst, Massachusetts 01003-9305, USA and Institut für Physik, Carl von Ossietzky Universität, D-26111 Oldenburg, Germany

Timothy P. Wiles[†] and Christoph Weiss[‡]
Joint Quantum Centre (JQC) Durham–Newcastle, Department of Physics, Durham University, Durham DH1 3LE, United Kingdom
(Received 20 September 2016; published 30 November 2016)

We model the dynamics of attractively interacting ultracold bosonic atoms in a quasi-one-dimensional wave guide with additional harmonic trapping. Initially, we prepare the system in its ground state and then shift the zero of the harmonic trap and switch on an additional narrow scattering potential near the center of the trap. After colliding with the barrier twice, we propose to measure the number of atoms opposite the initial condition. Quantum-enhanced interferometry with quantum bright solitons allows us to predict detection of an offset of the scattering potential with considerably increased precision as compared to single-particle experiments. In a future experimental realization this might lead to measurement of weak forces caused, for example, by small horizontal gradients in the gravitational potential—with a resolution of several micrometers given essentially by the size of the solitons. Our numerical simulations are based on the rigorously proved effective potential approach developed in previous papers [Phys. Rev. Lett. **102**, 010403 (2009) and Phys. Rev. Lett. **103**, 210402 (2009)]. We choose our parameters such that the prerequisite of the proof (that the solitons cannot break apart, for energetic reasons) is always fulfilled, thus exploring a parameter regime inaccessible to the mean-field description via the Gross-Pitaevskii equation due to Schrödinger-cat states occurring in the many-particle quantum dynamics.

DOI: 10.1103/PhysRevA.94.053638

I. INTRODUCTION

Matter-wave bright solitons can be used for interferometry by profiting from their mean-field description based on the Gross-Pitaevskii equation (GPE)—primarily by the fact that attractive interactions prevent the wave packets from spreading [1–5]. Matter-wave bright solitons[1] are investigated experimentally both for attractive interaction [3,7–15] and—in the presence of an optical lattice—also for repulsive interaction [16]. Recent experimental results for bright solitary waves in attractively interacting Bose-Einstein condensates include both a first step to interferometric applications [3] and collisions of two bright solitons [12] as well as quantum reflection off a narrow attractive potential barrier [13].

While current experiments can successfully be modeled by using the mean-field (GPE) approach, beyond-mean-field properties of quantum bright solitons are a focus of ongoing theoretical investigations [17–28]. In the current paper, we explore beyond mean-field many-particle quantum properties of matter-wave bright solitons [29,30] (cf. [27]) for interferometric purposes. While for mean-field based interferometry, quantum fluctuations in, for example, the center of mass velocity can endanger the interferometric scheme [31], in the present paper both interactions and quantum fluctuations are the tools to generate quantum-enhanced interferometry. While spin-squeezed states [32–37] are one possibility to achieve [38] quantum-enhanced interferometry, Schrödinger-cat states[2] are another [47–49] (cf. Ref. [50]). An experimental realization of an atom interferometer can be found in Ref. [51]; interferometry using nonentangled states leading to enhanced precision can be found in Ref. [52].

We use the rigorously proved [53] effective potential approach developed independently of each other in Refs. [21,22]. The effective potential approach is valid in the regime of low kinetic energies where the soliton is energetically forbidden to classically break apart, thus corresponding to a mean-field regime where reflection at a barrier leads to steps in the transmission coefficient [29,54,55].[3] In this energy regime both mesoscopic Schrödinger-cat states [21,29] and, for two-component Bose condensates, mesoscopic Bell states [58] have been predicted theoretically to occur in the many-particle quantum dynamics of quantum matter-wave bright solitons. For a single-species, attractively interacting Bose condensate and a repulsive barrier, the effective potential approach [21,22] is a powerful tool to model the many-particle quantum dynamics both for solitons of the order of $N = 100$ atoms [21] but also for much smaller particle numbers of $N = 2$ [59].

The paper is organized as follows: Section II describes how quantum bright solitons in one-dimensional wave guides

[*]b.gertjerenken@uni-oldenburg.de
[†]Now at Peratech http://www.peratech.com/
[‡]christoph.weiss@durham.ac.uk

[1]Our solitons are not solitons in the strict sense but rather solitary waves. However, these solitary waves can behave very similar to solitons [6].

[2]Schrödinger-cat states are discussed in Refs. [21,23,30,39–46] and references therein.

[3]In the regime of higher kinetic energy, where mean-field bright solitons do break apart when hitting a barrier, scattering has been investigated, for example, in Refs. [4,56,57] and references therein.

can be modeled; followed by the effective potential approach (Sec. III) we use to describe the many-particle quantum dynamics in the regime where matter-wave bright solitons are energetically forbidden to break apart. In Sec. IV we introduce the signature we propose to use for future experiments: the probability to find all particles on the side opposite to the initial condition after the soliton hits the barrier for the second time. In Sec. V we present our results: the quantum-enhancement achieved by using quantum bright solitons rather than single particles (or noninteracting Bose-Einstein condensates). The paper ends with conclusions and outlook in Sec. VI.

II. MODELING QUANTUM BRIGHT SOLITONS

In order to model attractively interacting atoms ($g_{1D} < 0$) in one dimension, the integrable Lieb-Liniger-(McGuire) Hamiltonian [60,61]

$$\hat{H} = -\sum_{j=1}^{N} \frac{\hbar^2}{2m} \frac{\partial^2}{\partial x_j^2} + \sum_{j=1}^{N-1} \sum_{n=j+1}^{N} g_{1D} \delta(x_j - x_n) \tag{1}$$

is available, where x_j denotes the position of particle j of mass m. The (attractive) interaction

$$g_{1D} = 2\hbar\omega_\perp a \tag{2}$$
$$< 0$$

is proportional to the s-wave scattering length a and the perpendicular angular trapping frequency $\omega_\perp$ [62]. Including the center-of-mass momentum K, the (internal) Lieb-Liniger ground state [19,61] reads (cf. [19])

$$\Psi(x_1, x_2, \ldots, x_N) \propto e^{iKX} \exp\left(-\frac{m|g_{1D}|}{2\hbar^2} \sum_{j<v} |x_j - x_v| \right); \tag{3}$$

the center-of-mass coordinate is given by

$$X = \frac{1}{N} \sum_{j=1}^{N} x_j. \tag{4}$$

The ground-state energy is given by

$$E_0(N, g_{1D}) = -\frac{m g_{1D}^2 N(N^2-1)}{24\hbar^2}. \tag{5}$$

Even more relevant for what we propose here, there is an energy gap between the internal ground state and the first excited state,

$$E_{gap} \equiv E_0(N-1) - E_0(N) \tag{6}$$
$$= \frac{m g_{1D}^2 N(N-1)}{8\hbar^2}. \tag{7}$$

As long as the total kinetic energy of the matter-wave bright soliton lies well within this energy gap,

$$E_{kin} < E_{gap}, \tag{8}$$

the validity of the effective potential approach of Refs. [21,22] can be proved rigorously [53]. This parameter-regime coincides with a complete breakdown of the validity of the Gross-Pitaevskii equation[4] for describing scattering matter-wave solitons off, for example, a narrow barrier [29,54,55,58].

If the center-of-mass wave function is a delta function and the particle number is $N \gg 1$, then the single-particle density can be shown [19,64] to be equivalent to the mean-field result based on the Gross-Pitaevskii equation [63] (cf. footnote 4)

$$\varrho(x) = \frac{N}{4\xi_N \{\cosh[x/(2\xi_N)]\}^2}, \tag{9}$$

normalized to the total number of particles N; the soliton length is given by

$$\xi_N \equiv \frac{\hbar^2}{m|g_{1D}|(N-1)}. \tag{10}$$

Adding a longitudinal harmonic trapping potential,

$$V(x_1, x_2, \ldots, x_N) = \sum_{j=1}^{N} V_0(x_j), \tag{11}$$
$$V_0(x) = \tfrac{1}{2} m\omega^2 (x + X_0)^2, \tag{12}$$

does not change the physics (beyond breaking integrability)—as long as [65] the soliton length is small compared to the harmonic oscillator length

$$\lambda_{HO} \equiv \sqrt{\frac{\hbar}{m\omega}}. \tag{13}$$

The plane waves in the center-of-mass coordinate in Eq. (3) become harmonic oscillator eigenfunctions in this limit [66]. After preparing the system in its ground state, at $t = 0$ the single-particle potential V_0 is changed quasi-instantaneously to

$$V_1(x) = \tfrac{1}{2} m\omega^2 x^2 + v_1 \delta(x - X_S), \tag{14}$$

thus moving the center of the longitudinal trap by X_0 and adding a very narrow scattering potential (modeled by a delta function) which is shifted by a distance of X_S from the trap center. As the proof of the validity of the effective potential approach introduced in the following section uses repulsive potentials [21,53] we choose $v_1 > 0$, where v_1 quantifies the strength of the scattering potential.

III. THE RIGOROUSLY PROVED EFFECTIVE POTENTIAL APPROACH

The effective potential method was developed independently by K. Sacha, C. A. Müller, D. Delande, and J. Zakrzewski [22] and C. Weiss and Y. Castin [21]. The rigorous mathematical proof by Y. Castin published a couple of years

[4] The mean-field approach via the Gross-Pitaevskii equation (GPE) [63]

$$i\hbar \frac{\partial}{\partial t}\varphi = -\frac{\hbar^2}{2m}\frac{\partial^2}{\partial x^2}\varphi + (N-1) g_{1D} |\varphi|^2 \varphi.$$

is a useful tool to explain ongoing state-of-the art experiments with matter-wave bright solitons like the experiments of Refs. [12,13]. However, the mean-field approach fails in the quantum regime [29,58] that makes the quantum-enhanced interferometry proposed in the current paper possible.

later [53] includes strict error bounds demonstrating that this is a highly reliable many-particle method in the energy regime where bright solitons cannot break apart for energetic reasons [Eq. (8)].

While this restricts the applicability to kinetic energies that lie within the energy gap between the internal ground state (all N particles in one soliton) and the internal first excited state ($N-1$ particles in one soliton), the effective potential is a high-end many-particle method that replaces the many-particle Schrödinger equation by an effective equation for the center-of-mass wave function in a nonperturbative way [53]. In cases where the center-of-mass wave function is localized at two places separated by more than the soliton length, this automatically corresponds to highly entangled Schrödinger-cat states.

In general, the effective potential is the convolution between the scattering potential and the soliton [21,22,53]. For the relevant single-particle potential (14) the result is particularly simple: The harmonic trap simply is replaced by a harmonic trap with identical trapping frequency but for a particle of mass mN; the delta function is replaced by the mean-field soliton profile (9) multiplied by the strength of the delta-function scattering potential v_1 (cf. Ref. [53]). As both potentials are a function of the center-of-mass coordinate, this leads to a further huge advantage of the effective potential approach: By introducing the effective potential, we have replaced the many-particle Schrödinger equation by an effective single-particle Schrödinger equation for the center of mass X with

$$i\hbar\frac{\partial}{\partial t}\varphi(X,t) = -\frac{\hbar^2}{2mN}\frac{\partial^2}{\partial X^2}\varphi(X,t) + V_{\rm eff}(X)\varphi(X,t), \quad E_{\rm kin} < E_{\rm gap}, \tag{15}$$

$$V_{\rm eff}(X) = \frac{1}{2}mN\omega^2X^2 + \frac{v_1N}{4\xi_N\{\cosh[(X-X_S)/(2\xi_N)]\}^2}. \tag{16}$$

The proof of the effective-potential approach requires that the kinetic energy is smaller than the energy gap (7) [21,53].

For sufficiently small ratio of soliton length to harmonic oscillator length, the effective potential can even be approximated by [29]

$$V_{\rm eff}(X) \simeq \tfrac{1}{2}mN\omega^2X^2 + v_1N\delta(X-X_S), \tag{17}$$

which could be treated analytically [67]. In the following section, our approach will be to combine an approximate analytical treatment of the scattering of the soliton off the potential with full numerics for which the center-of-mass wave function of the ground state soliton is prepared in the harmonic oscillator ground state. The trap is then shifted such that the soliton moves towards the new minimum—in which then a narrow scattering potential is switched on.

While the model displayed in Eqs. (15)–(17) looks like a single-particle approach, these equations for a particle of mass Nm describe many-particle quantum dynamics in the parameter regime in which quantum bright solitons cannot break apart [21,53] (cf. Ref. [22]). Any solution of Eq. (15) which spreads over more than the soliton width can thus be identified as being a mesoscopic quantum superposition [21] of the Schrödinger-cat type relevant for quantum-enhanced interferometry [47]. In the following, we will focus on 50:50 splitting leading to the particularly useful [47] high-fidelity Schrödinger-cat state. To identify more general quantum superpositions see, e.g., Ref. [68].

To summarize, thanks to the rigorous proof of Ref. [53], the effective potential approach is a highly reliable many-particle method for quantum bright solitons. Its level of reliability in the regime of low kinetic energies (in which the proof of Ref. [53] is valid) is at least as high as high-end many-particle methods used, for example, in Refs. [23,26] (cf. Refs. [69,70]). The occurrence of highly entangled Schrödinger-cat states relevant for quantum-enhanced interferometry [47,49] is thus guaranteed—under conditions that are within the reach of ongoing state-of-the-art experiments [11–14].

IV. EXPERIMENTALLY ACCESSIBLE SIGNATURE

We propose to prepare the ground state of N attractively interacting atoms in a one-dimensional wave guide with additional weak harmonic trapping. After quasi-instantaneously shifting the harmonic potential by several soliton lengths, we switch on a very narrow *repulsive* scattering potential in the center of the trap and observe the quantum dynamics for 50:50 splitting after the first collision for two collisions (cf. Refs. [29,30,45]). In Fig. 1 we compare what happens to a single atom ($N=1$) to a $N=100$ quantum bright soliton: In the limit that the effective potential behaves similar to a delta function, the length scales are a factor of 10 smaller for the $N=100$ soliton[5] compared to $N=1$. In passing we note that the signature demonstrated in Fig. 1(b) [and also in Fig. 3(c)] is not accessible on the mean-field (GPE) level as it involves intermediate Schrödinger-cat states[6] as the soliton is not energetically allowed to break into smaller parts, thus what is shown in Fig. 1(b) for times $t \approx 100$ ms corresponds to a quantum superposition of all particles being either on the left or right of the scattering potential. The main difference between the two panels of Fig. 1 is that the upper panel is only for one particle. While one might choose to call this a Schrödinger cat [39], if describing a noninteracting Bose-Einstein condensate with N particles in a rather classical product state, the following section shows that the state displayed in the upper panel lacks the many-particle entanglement properties

[5]For ^{7}Li and $N \approx 100$, the set of parameters used is the slightly modified parameter set (we doubled the strength of the radial trapping frequency) of Ref. [21] for the s-wave scattering length $a = -1.72 \times 10^{-9}$ m,$\omega_\perp = 2\pi \times 2 \times 4800$ Hz. In addition we chose $\omega = 2\pi \times 5$ Hz. The initial distance from the trap center is chosen to be $X_0 = 30\ \mu$m; this can easily be reduced for bright solitons (but not for single particles or weakly interacting Bose-Einstein condensates). For the soliton it corresponds to $E_{\rm kin}/|E_0(N)| \simeq 0.83$, within the regime of validity of the effective potential approach [cf. Eq.(17)].

[6]In the energy regime in which the many-particle quantum mechanics predicts Schrödinger-cat states, the GPE shows strong jumps [29,54,55] in the transmission behavior. When colliding with the scattering potential twice, the solitons are either reflected or transmitted in both cases. Thus, the GPE soliton ends on the same side as the initial condition (cf. Ref. [56]) and on the opposite side to the many-particle quantum prediction.

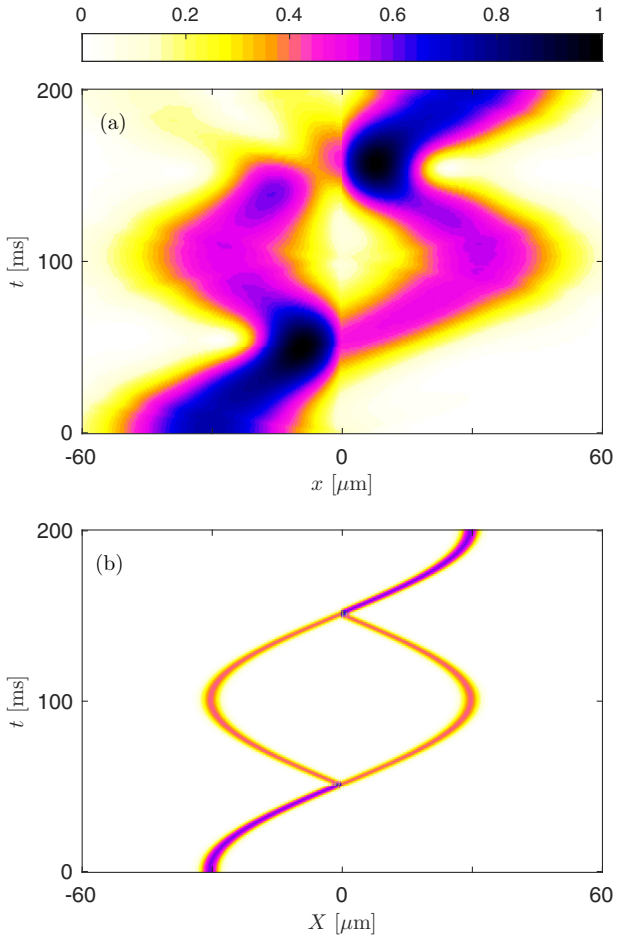

FIG. 1. As the experimentally accessible signature we suggest to use the probability to find all particles on the side opposite to the initial condition after scattering twice [shown is the two-dimensional projection of the modulus squared of the center-of-mass wave function as a function of both position and time for (a) $N = 1$ and (b) a $N = 100$ soliton for the parameters of footnote 5]. After being prepared in the ground state of a harmonic trap, at $t = 0$ the trap is shifted and a narrow *repulsive* scattering potential switched on at the new center of the trap. After the scattering potential is hit for the first time, Schrödinger-cat states occur; after the second collision all particles are on the side opposite to the initial condition (cf. Ref. [29]). The fact that Schrödinger-cat states occur is a consequence of the fact that slow bright solitons cannot energetically break apart (cf. Ref. [21], footnote 5); the interaction remains switched on the entire time.

necessary for quantum-enhanced interferometry for which the state displayed in the lower panel is particularly useful.

In order for the signature displayed in Fig. 1 to work, the timescale for decoherence events via, for example, single- or three-particle losses has to be large compared to the total time of the experiment from the first time the soliton hits the barrier to being detected at the side opposite to its initial condition. Reference [21] shows a possible parameter set for ^{7}Li, using conservative estimates for the loss rates (cf. [71]), thus justifying that using trapping frequencies in the direction of motion of the order of $\omega = 2\pi \times 10$ Hz is indeed justified.

Before we show how the signature displayed in Fig. 1 can be used for future experiments with quantum-enhanced measurements, we would like to stress again that the fact that we have Schrödinger cat states relies on strong attractive interaction preventing the soliton from breaking apart and thus allowing the rigorously proved [53] effective potential approach of Refs. [21,22] Eqs. (15)–(17) to be used. While often interaction is only present to generate entanglement, for the signature displayed in Fig. 1 to work it is furthermore essential to leave the interaction switched on the entire time—otherwise the feature that all particles end up opposite to their initial condition would not work.

V. QUANTUM-ENHANCED MEASUREMENT: BEYOND-CLASSICAL PRECISION

A. Overview of Sec. V

In this section, we use the mathematically rigorous effective potential approach (Sec. III) to show that we can obtain beyond-classical precision in interferometric measurements with quantum-bright solitons. The fact that we are in the regime of validity of the effective potential approach guarantees both the occurrence of a Schrödinger-cat state and ensures that this is not accessible to nonlinear physics (for the GPE in the regime of low kinetic energies, the soliton would either pass the barrier twice or be reflected twice, thus in both cases ending back in the original position rather than opposite to the initial position as shown for the quantum case in Fig. 1.

In Sec. V B we show that the signature to find all particles opposite to the initial condition oscillates as a function of the distance of barrier from the center of the trap (moved by a horizontal force) position [Eq. (20)] both by using an intuitive analytical approximation which is backed up by systematic numerical simulations. In Sec. V C we summarize the role Schrödinger cats play in our scheme and stress the role of measuring atoms in Bose-Einstein condensates via scattering or absorbing photons. Section V D shows how this is related to the precision: As described in Refs. [47,48] quantum-enhanced interferometry with Schrödinger-cat states gains a factor of N in the precision with which the phase can be detected. Repeating the single-particle experiment N times more often than the experiment with N-particle Schrödinger-cat state yields an overall win of a factor of $1/\sqrt{N}$ for the Schrödinger cats [Ref. [47], Sec. "Quantum-Enhanced Parameter Estimation"]. In Sec. V E we show how well horizontal differences in the gravitational field could be measured.

B. Dependence of the signature on the distance of the barrier from the trap center

As a practical example showing how much this improves the precision, we perform a thought measurement of a horizontal gradient in the gravitational potential, modeled as a linear potential added to Eq. (15),

$$V_{\text{gravity}}(X) = -XmN\Delta g_{\text{gravity}}, \tag{18}$$

which would lead to a shift of the zero of the harmonic trapping potential and thus to a nonvanishing distance

$$X_S = \frac{\Delta g_{\text{gravity}}}{\omega^2} \tag{19}$$

between trap center and scattering potential. In order to estimate the precision of our interferometric measurement, we need to determine the position of a maximum by repeating the measurements n times. The interference pattern as a function of X_S—namely the transmission coefficient after scattering at the potential twice—is given by the approximate analytical formula [29]

$$T = \tfrac{1}{2}[1 + \cos(4\Omega X_s)] \tag{20}$$

$$\Omega = \frac{Nm\omega X_0}{\hbar}. \tag{21}$$

In order to derive the last line, we used energy conservation to derive the center-of-mass momentum $\hbar K$ via

$$\frac{(\hbar K)^2}{2Nm} = \frac{1}{2}Nm\omega^2 X_0^2, \quad \text{and thus} \tag{22}$$

$$K = \frac{Nm\omega X_0}{\hbar}, \tag{23}$$

together with the textbook [72] result that scattering a particle of mass Nm with a plane wave with momentum $\hbar K$ from a delta function potential

$$V(X) = \frac{\hbar^2\Omega}{Nm}\delta(X) \tag{24}$$

leads to fifty-fifty splitting if

$$K = \Omega. \tag{25}$$

While the true effective potential will be broader than the delta function used here, this only affects the amplitude, not the spatial period of the oscillations [see Fig. 2(a), cf. [29] Fig. 3]. For the same parameters as the numerical data depicted in Fig. 2(b), Fig. 2(c) shows the analytical formula (20) confirming that this formula predicts the width of the interference patterns correctly. As predicted by Eq. (21), the spatial period increases for decreasing X_0 [see Fig. 2(b)]. Thus the delta-function approximation is sufficient for the purpose of estimating the precision of our interferometric setup.

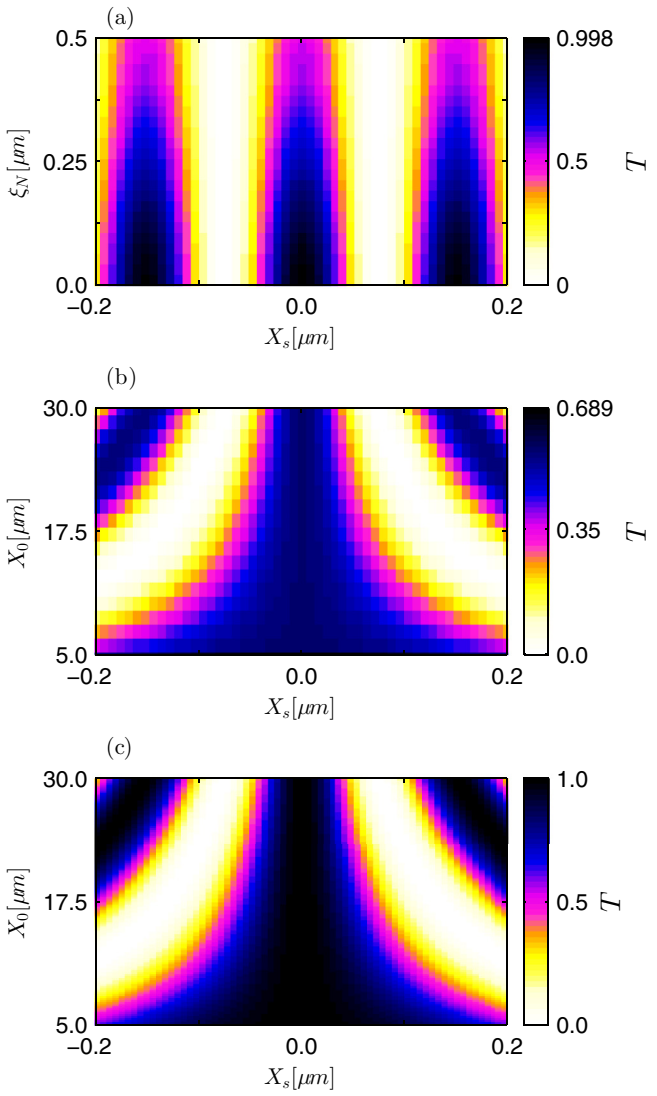

FIG. 2. (a) Our signature that everything is on the side opposite to the initial condition after colliding with the barrier twice, denoted by T, as a function of distance X_s between trap minimum and scattering potential for different widths of the $1/\cosh^2$ potential, introduced in Eq. (16), $X_0 = 30\ \mu$m and $N = 100$ particles. The value $\xi = 0.42\ \mu$m corresponds to the parameters from footnote 5. The limit $\xi \to 0$ corresponds to a delta function potential. (b) Same for varying initial displacements X_0 and $\xi = 0.42\ \mu$m kept fixed. (c) Displays the analytical result (20) for the same parameters as panel (b). Thus panel (c) confirms that the analytical approximation (20) qualitatively correctly captures the physics displayed in the many-particle quantum dynamics of panel (b).

C. Role of Schrödinger-cat states and measuring particles in a BEC

The signature we use for our interferometry scheme relies on a very fundamental level on Schrödinger-cat states: After two collisions with a barrier, neither the numerical results for the transmission after two collisions with a barrier depicted in Fig. 2 nor the analytic result of Eq. (20) could have been obtained with a mean-field description via the GPE. In the regime of low kinetic energies in which the rigorously derived effective potential approach is valid (see Sec. III, [21,22,53]), the GPE predicts unphysical jumps in the transmission/reflection behavior [29,54,55]; solitons would be either reflected twice or transmitted twice, in both cases ending up at the same side of the scattering potential for the two collisions investigated here, corresponding to the mean-field (GPE) prediction

$$T_{\text{GPE}} = 0. \tag{26}$$

Rewriting Eq. (20) to show the N dependence explicitly,

$$T = \frac{1}{2}\left[1 + \cos\left(N\frac{4m\omega X_0 X_S}{\hbar}\right)\right], \tag{27}$$

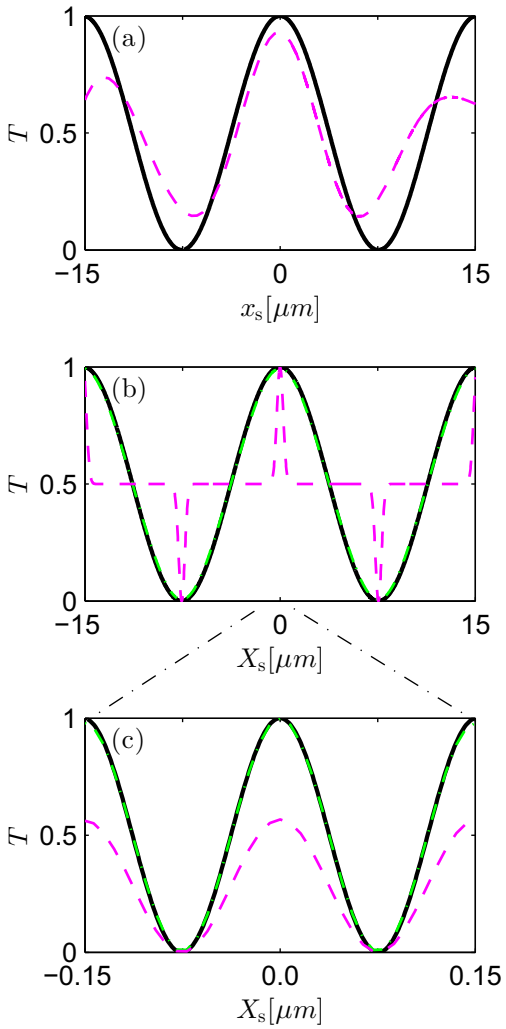

FIG. 3. Our signature that everything is on the side opposite to the initial condition after colliding with the barrier twice as a function of distance between trap minimum and scattering potential [see. Fig. 1 also for parameters used] for (a) a single particle: numerical data [magenta (dark gray) dashed curve] and analytical formula (20) (black solid curve) and (b) repeating the experiment 100 times with single particles [magenta (dark gray) dashed curve] compared to the single-particle result (20) (black solid curve) and replacing this result by a combination of Gaussians [green (light gray) dash-dotted curve]. (c) Shows quantum enhancement by a factor of $1/\sqrt{N}$ for a quantum bright soliton of $N = 100$. Shown are formula (20) (black solid curve), numerical data using a delta-function barrier [green (light gray) dash-dotted curves], and the $1/\cosh^2$ potential corresponding to the parameters of footnote 5 [magenta (dark gray) dashed curve].

yields a reduction of the width of the interference patterns by a factor of N. This is identical to the general case discussed in [Ref. [47], Sec. "Quantum-Enhanced Parameter Estimation"] when replacing a single-particle quantum superposition by an N-particle Schrödinger cat, the first step towards quantum-enhanced interferometry.

Observations of atomic Bose-Einstein condensates employ scattering or absorption of laser light [73]. Multiple scattering let alone absorption of the same photon are not an issue that is discussed in such cases [73], a fact that is further stressed by the small atom numbers $N \approx 100$ which are the focus of our current paper. Thus, measuring a BEC of N noninteracting atoms is equivalent to measuring N single atoms independently. In both cases, the central limit theorem thus increases the precision by a factor of $1/\sqrt{N}$.

Note that if measuring the Schrödinger-cat state, an individual measurement of T is either 0 or N. While having N atoms in a bright soliton can simplify detecting it, there is no additional correction corresponding to the factor $1/\sqrt{N}$. To determine the precision, in Sec. V D we repeat the above thought experiment n times (comparing an noninteracting BEC with the bright soliton Schrödinger-cat state).

D. Precision

In order to answer how precisely we can determine the position of the scattering potential with respect to the trap center, we have to consider a couple of separate points. All are based on the distance between minima/maxima, as determined by Eq. (20). Half the distance between two minima is given by

$$\Delta X_S = \frac{\pi}{4\Omega} \tag{28}$$

$$= \frac{1}{N}\frac{\pi\hbar}{2m\omega X_0}. \tag{29}$$

(1) The aim is to move the scattering potential back to the center when it was moved by a small distance from there; thus our device will have to remember by how much the potential has moved.

(2) Repeating the experiment n times for various distances will give us a part of the cosine of Eq. (20) centered around the maximum.

(3) Half the distance between two minima gives a first order of magnitude of the precision with which we can measure the position; the larger the particle number in our soliton the higher the precision will be. (In an actual experiment, the full width at half maximum could be used equivalently).

(4) If measured in terms of the precision that can be read off the distance of the interference fringes, a quantum-enhanced measurement is better by a factor of $1/N$. This is the typical scaling for quantum-enhanced interferometers with Schrödinger-cat states as compared to single particles [[48], Fig. 1]. This difference of a factor of N is visible by comparing Figs. 3(a) and 3(c).

(5) In our case, the increased precision described in point V D above is related to the de Broglie wavelength of the particles, smaller wavelengths allowing us to measure smaller distances. Thus, this is independent of precise details of the initial state.

(6) Repeating the quantum-enhanced measurement n times with Schrödinger-cat states of N atoms in order to determine the position of the maximum involves $n \times N$ atoms.

(7) In order to compare the outcome with the single-particle case (cf. [48]) thus repeat the same interferometric sequence of measuring the position of the maximum with single particles $n \times N$ times. Compared to the quantum-enhanced case, this increases the number of measurements by a factor of N, allowing us to determine the position of the maximum more precisely. As the errors involved in repeating such experiments N times more often scale as $1/\sqrt{N}$ [[47],

Sec. "Quantum-Enhanced Parameter Estimation"],

$$\delta X_{N\text{noninteracting particles}} \propto \frac{\delta X_{N=1\text{ noninteracting particle}}}{\sqrt{N}}, \tag{30}$$

we thus have

$$\delta X_{N-\text{particle soliton}} \propto \frac{\delta X_{N\text{ noninteracting particles}}}{\sqrt{N}} \tag{31}$$

$$\propto \frac{\delta X_{N=1\text{ noninteracting particle}}}{N}. \tag{32}$$

Thus, to summarize, the precision of the single-particle case is limited by the Heisenberg-uncertainty relation [the distance measured (29) is of the order of the de Broglie wavelength; independent of the precise initial state, the momentum is of the order of $m\omega X_0$]. The minimal distance measurable can be improved by statistical analysis of repeating the experiment N times, giving an improvement of a factor of $1/\sqrt{N}$ for the smallest distance that can be measured [Eq. (30)] for repeated experiments with single particles [[47], Sec. "Quantum-Enhanced Parameter Estimation"]. A precision which scales faster with N as displayed in Eq. (32) thus seems, at first glance, to violate the Heisenberg uncertainty relation.

However, many-particle entangled states like Schrödinger-cat states are known to show such behavior which is sometimes described as "beating the standard quantum limit" [47]. As the de Broglie wavelengths are a factor of N smaller than for the single-particle case, it should not be surprising that we can measure distances with the precision of Eq. (32). The overall gain of a factor of $1/\sqrt{N}$ is of course consistent with the Heisenberg-uncertainty relation if applied to our N-particle Schrödinger-cat state (cf. [47,48]).

While the analytical calculations are based on the approximate result given in Eq. (20), the oscillation periods are confirmed by doing full numerics (Figs. 2 and 3): In panel Fig. 3(a), the full numerical result shows that it is straightforward to identify the position of the maximum. Combining the central-limit theorem with the analytical approximation using Gaussians demonstrates that repeating the experiment 100 times will lead to an increased precision for the position of the maximum of a factor of 10 [Fig. 3(b)]. While the numerics using the delta function agree with the analytic predictions of Eq. (20), for the $1/\cosh^2$ potential corresponding to the parameters of footnote 5 the amplitude is smaller.

E. Measuring horizontal differences in the gravitational potential

Thus, our thought experiment can measure differences in the gravitational acceleration of at least

$$|\Delta g_{\text{gravity}}| < \omega^2 \Delta X_{\text{S}}, \tag{33}$$

which yields a difference in acceleration of

$$|\Delta g_{\text{gravity}}| < \frac{1}{N}\frac{\pi\omega\hbar}{2mX_0}. \tag{34}$$

This yields a difference in the acceleration potential of

$$2X_0|\Delta g_{\text{gravity}}| < \frac{1}{N}\frac{\pi\omega\hbar}{m}, \tag{35}$$

which takes into account the fact that we effectively average $\Delta g_{\text{gravity}}$ over a distance $2X_0$. Thus, within the definition (35), the precision is independent of our choice of X_0. The strength of quantum bright solitons lies in particular in the fact that one can get much closer to the scattering potential than for noninteracting particles, thus exploring shorter length scales.

For ^{7}Li, $N = 100$ (cf. [21], footnote 5) and $\omega = 2\pi \times 5$ Hz, if our thought experiment involves measuring n solitons, it can detect differences smaller than $(0.009/\sqrt{n})\ \mu\text{m m/s}^2$. By replacing ^{7}Li by ^{85}Rb we could gain another order of magnitude in precision. While at first glance it might appear to be tempting to propose to both further reduce the trapping frequency and further increase the particle number, the validity of Eq. (35) relies on the occurrence of intermediate Schrödinger-cat states and thus will work better for not too large particle numbers and not too long timescales.

Depending on the magnitude of the potential differences we intend to measure on micrometer scale (gravity was just an example), the precision might actually be too large to easily determine the distance of the scattering potential from the trap center. To work out a clever way to start with reduced precision (with noninteracting atoms and/or higher trapping frequencies) in order to roughly determine the position and to continuously increase the precision could still be an engineering challenge. Nevertheless, our results clearly indicate the feasibility of such a device.

VI. CONCLUSION AND OUTLOOK

Similar to the case of the spin-squeezed states realized in the experiment of Ref. [38] demonstrating interferometric precision surpassing what is possible classically, Schrödinger-cat states can also be used for quantum-enhanced measurements [47,48] (cf. [49]). Quantum bright solitons generated from attractively interacting Bose gases are an ideal system to produce such Schrödinger-cat states [21]; state-of-the art experimental setups with ultracold atoms [11–14] could reach such a regime in the near future. Ultracold atoms can be applied to questions not easily accessible to photon experiments (cf. [74]).

In the present paper, we propose to use small, harmonically trapped quantum matter-wave bright solitons for quantum-enhanced measurements. The signature we propose to measure—the probability to find all particles at the side opposite to the initial condition—is not accessible on the mean-field (GPE) level as it involves intermediate Schrödinger-cat states (see footnote 6).

Our numerical simulations are done using the effective potential approach of Refs. [21,22] by taking care that the prerequisite of the proof [53] is fulfilled: The solitons are energetically forbidden to break apart. Thus, if the center-of-mass wave function is split 50:50 when the soliton hits the barrier for the first time, we are certain to have a Schrödinger-cat state. For the second step to work (that after recombining at the barrier the soliton ends at the side opposite to the initial condition), it is furthermore essential to maintain the quantum superposition [29]. While experimentally observing the motion of quantum bright solitons in the presence of decoherence via atom losses [75] would also be an interesting experiment, the quantum-enhanced interferometry will only work if decoherence via particle losses happens on timescales longer than the duration of the experiment (cf. [21]).

When shifting the position of the scattering potential away from the center, our signature oscillates. The spatial oscillation period scales $\propto 1/\sqrt{N}$ with the number of particles, thus providing the "usual" increase in precision by a factor of $1/\sqrt{N}$ quantum-enhanced measurements can provide. Here, it occurs when the position of the maximum is determined via repeated measurements.

A potential experimental realization of such a setup might be useful to measure small horizontal gradients in the gravitational force on micrometer scales in an approach complementary to existing experiments combining Bose-Einstein condensates and gravity [76]. The data presented in this paper are available online [77].

ACKNOWLEDGMENTS

We thank R. J. Bettles, T. P. Billam, S. L. Cornish, S. A. Gardiner, S. A. Hopkins, R. G. Hulet, and L. Khaykovich for discussions. B.G. thanks the European Union for funding through FP7-PEOPLE-2013-IRSES Grant No. 605096. C.W. thanks the Engineering and Physical Sciences Research Council UK (Grant No. EP/L010844/1) for funding. The computations were performed on the HPC cluster HERO, located at the University of Oldenburg and funded by the DFG through its Major Research Instrumentation Programme (INST 184/108-1 FUGG), and by the Ministry of Science and Culture (MWK) of Lower Saxony, Germany.

[1] A. D. Martin and J. Ruostekoski, Quantum dynamics of atomic bright solitons under splitting and recollision, and implications for interferometry, New J. Phys. **14**, 043040 (2012).

[2] J. Polo and V. Ahufinger, Soliton-based matter-wave interferometer, Phys. Rev. A **88**, 053628 (2013).

[3] G. D. McDonald, C. C. N. Kuhn, K. S. Hardman, S. Bennetts, P. J. Everitt, P. A. Altin, J. E. Debs, J. D. Close, and N. P. Robins, Bright Solitonic Matter-Wave Interferometer, Phys. Rev. Lett. **113**, 013002 (2014).

[4] J. L. Helm, S. L. Cornish, and S. A. Gardiner, Sagnac Interferometry Using Bright Matter-Wave Solitons, Phys. Rev. Lett. **114**, 134101 (2015).

[5] H. Sakaguchi and B. A. Malomed, Matter-wave soliton interferometer based on a nonlinear splitter, New J. Phys. **18**, 025020 (2016).

[6] A. D. Martin, C. S. Adams, and S. A. Gardiner, Bright solitary-matter-wave collisions in a harmonic trap: Regimes of solitonlike behavior, Phys. Rev. A **77**, 013620 (2008).

[7] L. Khaykovich, F. Schreck, G. Ferrari, T. Bourdel, J. Cubizolles, L. D. Carr, Y. Castin, and C. Salomon, Formation of a matter-wave bright soliton, Science **296**, 1290 (2002).

[8] K. E. Strecker, G. B. Partridge, A. G. Truscott, and R. G. Hulet, Formation and propagation of matter-wave soliton trains, Nature (London) **417**, 150 (2002).

[9] S. L. Cornish, S. T. Thompson, and C. E. Wieman, Formation of Bright Matter-Wave Solitons during the Collapse of Attractive Bose-Einstein Condensates, Phys. Rev. Lett. **96**, 170401 (2006).

[10] A. L. Marchant, T. P. Billam, T. P. Wiles, M. M. H. Yu, S. A. Gardiner, and S. L. Cornish, Controlled formation and reflection of a bright solitary matter-wave, Nat. Commun. **4**, 1865 (2013).

[11] P. Medley, M. A. Minar, N. C. Cizek, D. Berryrieser, and M. A. Kasevich, Evaporative Production of Bright Atomic Solitons, Phys. Rev. Lett. **112**, 060401 (2014).

[12] J. H. V. Nguyen, P. Dyke, D. Luo, B. A. Malomed, and R. G. Hulet, Collisions of matter-wave solitons, Nat. Phys. **10**, 918 (2014).

[13] A. L. Marchant, T. P. Billam, M. M. H. Yu, A. Rakonjac, J. L. Helm, J. Polo, C. Weiss, S. A. Gardiner, and S. L. Cornish, Quantum reflection of bright solitary matter waves from a narrow attractive potential, Phys. Rev. A **93**, 021604(R) (2016).

[14] P. J. Everitt, M. A. Sooriyabandara, G. D. McDonald, K. S. Hardman, C. Quinlivan, M. Perumbil, P. Wigley, J. E. Debs, J. D. Close, C. C. N. Kuhn, and N. P. Robins, arXiv:1509.06844.

[15] S. Lepoutre, L. Fouché, A. Boissé, G. Berthet, G. Salomon, A. Aspect, and T. Bourdel, arXiv:1609.01560.

[16] B. Eiermann, Th. Anker, M. Albiez, M. Taglieber, P. Treutlein, K.-P. Marzlin, and M. K. Oberthaler, Bright Bose-Einstein Gap Solitons of Atoms with Repulsive Interaction, Phys. Rev. Lett. **92**, 230401 (2004).

[17] S. J. Carter, P. D. Drummond, M. D. Reid, and R. M. Shelby, Squeezing of Quantum Solitons, Phys. Rev. Lett. **58**, 1841 (1987).

[18] Y. Lai and H. A. Haus, Quantum theory of solitons in optical fibers. ii. exact solution, Phys. Rev. A **40**, 854 (1989).

[19] Y. Castin and C. Herzog, Bose-Einstein condensates in symmetry breaking states, C. R. Acad. Sci. Paris, Ser. IV **2**, 419 (2001).

[20] L. D. Carr and J. Brand, Spontaneous Soliton Formation and Modulational Instability in Bose-Einstein Condensates, Phys. Rev. Lett. **92**, 040401 (2004).

[21] C. Weiss and Y. Castin, Creation and Detection of a Mesoscopic Gas in a Nonlocal Quantum Superposition, Phys. Rev. Lett. **102**, 010403 (2009).

[22] K. Sacha, C. A. Müller, D. Delande, and J. Zakrzewski, Anderson Localization of Solitons, Phys. Rev. Lett. **103**, 210402 (2009).

[23] A. I. Streltsov, O. E. Alon, and L. S. Cederbaum, Efficient generation and properties of mesoscopic quantum superposition states in an attractive Bose-Einstein condensate threaded by a potential barrier, J. Phys. B **42**, 091004 (2009).

[24] P. Bienias, K. Pawlowski, M. Gajda, and K. Rzazewski, Statistical properties of one-dimensional attractive Bose gas, EPL (Europhys. Lett.) **96**, 10011 (2011).

[25] A. I. Streltsov, O. E. Alon, and L. S. Cederbaum, Swift Loss of Coherence of Soliton Trains in Attractive Bose-Einstein Condensates, Phys. Rev. Lett. **106**, 240401 (2011).

[26] L. Barbiero, B. A. Malomed, and L. Salasnich, Quantum bright solitons in the Bose-Hubbard model with site-dependent repulsive interactions, Phys. Rev. A **90**, 063611 (2014).

[27] O. I. Streltsova and A. I. Streltsov, arXiv:1412.4049.

[28] B. Gertjerenken and P. G. Kevrekidis, Effects of interactions on the generalized Hong-Ou-Mandel effect, Phys. Lett. A **379**, 1737 (2015).

[29] B. Gertjerenken, T. P. Billam, L. Khaykovich, and C. Weiss, Scattering bright solitons: Quantum versus mean-field behavior, Phys. Rev. A **86**, 033608 (2012).
[30] B. Gertjerenken, Bright-soliton quantum superpositions: Signatures of high- and low-fidelity states, Phys. Rev. A **88**, 053623 (2013).
[31] J. L. Helm, S. J. Rooney, C. Weiss, and S. A. Gardiner, Splitting bright matter-wave solitons on narrow potential barriers: Quantum to classical transition and applications to interferometry, Phys. Rev. A **89**, 033610 (2014).
[32] J. K. Korbicz, J. I. Cirac, and M. Lewenstein, Spin Squeezing Inequalities and Entanglement of *n* Qubit States, Phys. Rev. Lett. **95**, 120502 (2005).
[33] R. Schnabel, Gravitational wave detectors: Squeezing up the sensitivity, Nat. Phys. **4**, 440 (2008).
[34] Y. Li, Y. Castin, and A. Sinatra, Optimum Spin Squeezing in Bose-Einstein Condensates with Particle Losses, Phys. Rev. Lett. **100**, 210401 (2008).
[35] G. Ferrini, A. Minguzzi, and F. W. J. Hekking, Number squeezing, quantum fluctuations, and oscillations in mesoscopic Bose Josephson junctions, Phys. Rev. A **78**, 023606 (2008).
[36] J. Esteve, C. Gross, A. Weller, S. Giovanazzi, and M. K. Oberthaler, Squeezing and entanglement in a Bose-Einstein condensate, Nature (London) **455**, 1216 (2008).
[37] L. I. R. Gil, R. Mukherjee, E. M. Bridge, M. P. A. Jones, and T. Pohl, Spin Squeezing in a Rydberg Lattice Clock, Phys. Rev. Lett. **112**, 103601 (2014).
[38] C. Gross, T. Zibold, E. Nicklas, J. Esteve, and M. K. Oberthaler, Nonlinear atom interferometer surpasses classical precision limit, Nature (London) **464**, 1165 (2010).
[39] C. Monroe, D. M. Meekhof, B. E. King, and D. J. Wineland, A "Schrödinger cat" superposition state of an atom, Science **272**, 1131 (1996).
[40] J. A. Dunningham and K. Burnett, Proposals for creating Schrodinger cat states in Bose-Einstein condensates, J. Mod. Opt. **48**, 1837 (2001).
[41] J. Dunningham, A. Rau, and K. Burnett, From pedigree cats to fluffy-bunnies, Science **307**, 872 (2005).
[42] M. A. García-March, D. R. Dounas-Frazer, and L. D. Carr, Macroscopic superposition of ultracold atoms with orbital degrees of freedom, Phys. Rev. A **83**, 043612 (2011).
[43] X.-C. Yao, T.-X. Wang, P. Xu, H. Lu, G.-S. Pan, X.-H. Bao, C.-Z. Peng, C.-Y. Lu, Y.-A. Chen, and J.-W. Pan, Observation of eight-photon entanglement, Nat. Photonics **6**, 225 (2012).
[44] L. Dell'Anna, Analytical approach to the two-site Bose-Hubbard model: From Fock states to Schrödinger cat states and entanglement entropy, Phys. Rev. A **85**, 053608 (2012).
[45] T. Fogarty, A. Kiely, S. Campbell, and T. Busch, Effect of interparticle interaction in a free-oscillation atomic interferometer, Phys. Rev. A **87**, 043630 (2013).
[46] U. R. Fischer and M.-K. Kang, "Photonic" Cat States from Strongly Interacting Matter Waves, Phys. Rev. Lett. **115**, 260404 (2015).
[47] V. Giovannetti, S. Lloyd, and L. Maccone, Quantum-enhanced measurements: Beating the standard quantum limit, Science **306**, 1330 (2004).
[48] V. Giovannetti, S. Lloyd, and L. Maccone, Advances in quantum metrology, Nat. Photon. **5**, 222 (2011).
[49] J. Chwedeńczuk, F. Piazza, and A. Smerzi, Phase estimation from atom position measurements, New J. Phys. **13**, 065023 (2011).
[50] S. L. Braunstein and C. M. Caves, Statistical Distance and the Geometry of Quantum States, Phys. Rev. Lett. **72**, 3439 (1994).
[51] S. Dimopoulos, P. W. Graham, J. M. Hogan, and M. A. Kasevich, Testing General Relativity with Atom Interferometry, Phys. Rev. Lett. **98**, 111102 (2007).
[52] S. Boixo, A. Datta, M. J. Davis, S. T. Flammia, A. Shaji, and C. M. Caves, Quantum Metrology: Dynamics versus Entanglement, Phys. Rev. Lett. **101**, 040403 (2008).
[53] C. Weiss and Y. Castin, Elastic scattering of a quantum matter-wave bright soliton on a barrier, J. Phys. A **45**, 455306 (2012).
[54] C.-H. Wang, T.-M. Hong, R.-K. Lee, and D.-W. Wang, Particle-wave duality in quantum tunneling of a bright soliton, Opt. Express **20**, 22675 (2012).
[55] S. Damgaard Hansen, N. Nygaard, and K. Mølmer, arXiv:1210.1681.
[56] J. Cuevas, P. G. Kevrekidis, B. A. Malomed, P. Dyke, and R. G. Hulet, Interactions of solitons with a Gaussian barrier: splitting and recombination in quasi-one-dimensional and three-dimensional settings, New J. Phys. **15**, 063006 (2013).
[57] V. Dunjko and M. Olshanii, arXiv:1501.00075.
[58] B. Gertjerenken, T. P. Billam, C. L. Blackley, C. R. Le Sueur, L. Khaykovich, S. L. Cornish, and C. Weiss, Generating Mesoscopic Bell States via Collisions of Distinguishable Quantum Bright Solitons, Phys. Rev. Lett. **111**, 100406 (2013).
[59] B. Gertjerenken and C. Weiss, Nonlocal quantum superpositions of bright matter-wave solitons and dimers, J. Phys. B **45**, 165301 (2012).
[60] E. H. Lieb and W. Liniger, Exact analysis of an interacting Bose gas. I. The general solution and the ground state, Phys. Rev. **130**, 1605 (1963).
[61] J. B. McGuire, Study of exactly soluble one-dimensional N-body problems, J. Math. Phys. **5**, 622 (1964).
[62] M. Olshanii, Atomic Scattering in the Presence of an External Confinement and a Gas of Impenetrable Bosons, Phys. Rev. Lett. **81**, 938 (1998).
[63] C. J. Pethick and H. Smith, *Bose-Einstein Condensation in Dilute Gases* (Cambridge University Press, Cambridge, 2008).
[64] F. Calogero and A. Degasperis, Comparison between the exact and Hartree solutions of a one-dimensional many-body problem, Phys. Rev. A **11**, 265 (1975).
[65] Y. Castin, Internal structure of a quantum soliton and classical excitations due to trap opening, Eur. Phys. J. B **68**, 317 (2009).
[66] D. I. H. Holdaway, C. Weiss, and S. A. Gardiner, Quantum theory of bright matter-wave solitons in harmonic confinement, Phys. Rev. A **85**, 053618 (2012).
[67] T. Busch, B.-G. Englert, K. Rzazewski, and M. Wilkens, Two cold atoms in a harmonic trap, Found. Phys. **28**, 549 (1998).
[68] R. Bach and K. Rzążewski, Correlations in Atomic Systems: Diagnosing Coherent Superpositions, Phys. Rev. Lett. **92**, 200401 (2004).
[69] J. Major, M. Łącki, and J. Zakrzewski, Reexamination of the variational Bose-Hubbard model, Phys. Rev. A **89**, 043626 (2014).
[70] J. G. Cosme, C. Weiss, and J. Brand, Center-of-mass motion as a sensitive convergence test for variational multi-mode quantum dynamics, Phys. Rev. A **94**, 043603 (2016).

[71] Z. Shotan, O. Machtey, S. Kokkelmans, and L. Khaykovich, Three-Body Recombination at Vanishing Scattering Lengths in an Ultracold Bose Gas, Phys. Rev. Lett. **113**, 053202 (2014).

[72] S. Flügge, *Rechenmethoden der Quantentheorie* (Springer, Berlin, 1990).

[73] D. M. Stamper-Kurn and W. Ketterle, Spinor Condensates and Light Scattering from Bose-Einstein Condensates, in *Coherent Atomic Matter Waves*, edited by R. Kaiser, C. Westbrook, and F. David (Springer, Berlin, Heidelberg, 2001), Vol. 72, p. 139.

[74] M. O. Scully and J. P. Dowling, Quantum-noise limits to matter-wave interferometry, Phys. Rev. A **48**, 3186 (1993).

[75] C. Weiss, S. A. Gardiner, and H.-P. Breuer, From short-time diffusive to long-time ballistic dynamics: The unusual center-of-mass motion of quantum bright solitons, Phys. Rev. A **91**, 063616 (2015).

[76] H. Müntinga, H. Ahlers, M. Krutzik, A. Wenzlawski, S. Arnold, D. Becker, K. Bongs, H. Dittus, H. Duncker, N. Gaaloul, C. Gherasim, E. Giese, C. Grzeschik, T. W. Hänsch, O. Hellmig, W. Herr, S. Herrmann, E. Kajari, S. Kleinert, C. Lämmerzahl, W. Lewoczko-Adamczyk, J. Malcolm, N. Meyer, R. Nolte, A. Peters, M. Popp, J. Reichel, A. Roura, J. Rudolph, M. Schiemangk, M. Schneider, S. T. Seidel, K. Sengstock, V. Tamma, T. Valenzuela, A. Vogel, R. Walser, T. Wendrich, P. Windpassinger, W. Zeller, T. van Zoest, W. Ertmer, W. P. Schleich, and E. M. Rasel, Interferometry with Bose-Einstein Condensates in Microgravity, Phys. Rev. Lett. **110**, 093602 (2013).

[77] B. Gertjerenken, T. P. Wiles, and C. Weiss, http://dx.doi.org/10.15128/r2ft848q6, https://collections.durham.ac.uk/files/r2ft848q60b (2016), Progress towards quantum-enhanced interferometry with harmonically trapped quantum matter-wave bright solitons: Supporting data V2.